Calibration of nearshore process models—application of a hybrid genetic algorithm

B. G. Ruessink

ABSTRACT

The physically realistic functions implemented in nearshore process models are governed by parameters that usually do not represent measurable attributes of the nearshore and, therefore, need to be determined through calibration. The classical approach to calibrate nearshore process models is via manual parameter adjustments and visual comparisons of model predictions and measurements. In this paper a hybrid genetic algorithm, comprising a global population-evolution-based search strategy and a local Nelder–Mead simplex search, is used to calibrate nearshore process models in an objective and automatic manner. The effectiveness of the algorithm to find the optimum parameter setting are examined in two case studies with increasing complexity: a simple alongshore current model and a more complex cross-shore bed evolution model. Whereas the algorithm is found to be an effective method to find the optimum setting of the alongshore current model, it fails to identify the optimum parameter values in the bed evolution model, related to the strong interaction between two of the parameters in the suspended sediment transport equation. Setting one of the interdependent parameters to a constant value within its feasible space while retaining the other in the optimization procedure is found to be a feasible solution to the ill-posed optimization problem of the bed evolution model.

Key words | calibration, genetic algorithm, nearshore, optimization, physically based simulation modelling

B. G. Ruessink
Department of Physical Geography,
Faculty of Geosciences,
Institute for Marine and Atmospheric Research Utrecht,
Utrecht University,
PO Box 80.115,
3508 TC Utrecht,
The Netherlands
Tel: +31 30 2532405
Fax: +31 30 2531145
E-mail: *g.ruessink@geog.uu.nl*

NOTATION

a	lower bound of a parameter
b	upper bound of a parameter
f	factor used in non-uniform mutation
F	value of objective function (simple least squares)
$\bar{F}$	population-average F
F_b	best F in a population
F_r	regularization term that can be added to F
i	population number
i_{max}	maximum number of populations
j	integer
k_a	apparent roughness
k_c	current-related roughness
k_w	wave-related roughness
m	chance of selecting the best individual into the next population
m'	normalization factor
M	probability in normalized geometric ranking
n	number of individuals
N_c	number of crossover operations
N_n	number of mutation operations
N_p	number of model parameters
N_t	number of temporal observations
N_x	number of cross-shore positions
p	individual in a population
P	population
r	rank
t	time
x	cross-shore coordinate
u	uniform random number between 0 and 1
$\bar{v}$	alongshore current velocity
X^{obs}	observation (in general)
X^{mod}	model result (in general)

β	roller slope	θ_0	best prior estimate of θ
Γ	covariance matrix that represents the uncertainty in θ	ν	eddy viscosity
		σ	standard deviation of F
θ	vector of model parameters	ϕ	angle of repose

INTRODUCTION

Nearshore process models are designed to resemble the physical processes that govern nearshore hydrodynamics, sediment transport and/or bathymetric evolution. The physically realistic functions implemented in these models are usually heuristically or (semi-) empirically determined and are governed by parameters. Ideally, these parameters have meaning outside the context of the model, which implies that the values of the parameters can be measured independently and do not need to be obtained through model calibration. However, many parameters do not represent measurable attributes in the nearshore; also, in cases where measured values do exist, they often differ from model calibrated values and may even show opposite trends (see, for an example, Ruessink *et al.* 2003). For any nearshore model to have (practical) applicability, model calibration seems to be the only feasible procedure to determine the proper (but, potentially, unrealistic) values of the governing parameters.

The calibration of nearshore process models is a non-linear optimization problem. The presently most-often adopted approach of nearshore model optimization is manual calibration, which involves numerous trial-and-error parameter adjustments and visual comparisons of the match between the observed and modelled variable(s) of interest. Even though a model expert can obtain excellent results, manual calibration is often time-consuming, labour-intensive and subjective, and does not provide any knowledge as to whether the best fit parameter values have actually been obtained.

The alternative to manual calibration is automatic calibration. An optimization algorithm iteratively searches the response surface (in parameter space) of an objective measure of the goodness of fit between observations and model predictions (the so-called objective function) for the parameter values that optimize this objective function. Many different algorithms exist (see, for example, Duan (2003) for an overview), each of which has its own set of rules on how the parameter values are optimized (henceforth, it is assumed minimized) as efficient (computational burden) and effective (success in finding the global minimum) as possible. Local search methods, which start their search for the optimum values with a single initial parameter guess and use local information only to determine a promising direction towards a minimum, are particularly useful when the response surface is unimodal. On a multi-modal response surface, local search methods fail as they may become trapped in a local minimum rather than converge to the global minimum (e.g. Duan *et al.* 1992). Even if the response function is expected to be unimodal, a number of local-search runs with different randomly selected initial guesses need to be carried out to investigate whether the objective function indeed contains a single minimum. Only if all trials converge to the same minimum can one be sure to have found the global minimum. The use of multiple runs has turned the optimization into a global search method known as the multistart approach (e.g. Duan *et al.* 1992). This is, however, an inefficient approach as each local search operates independently because it does not share any information with the other searches. One way of improving global optimization efficiency through information sharing is the use of genetic algorithms (GAs) (Holland 1975). A GA maintains a population of potential solutions, which through probabilistic manipulation (selection, cross-over (mating) and mutation) and a survival of the fittest strategy evolve to solutions close to the global minimum. Because the initial population can be chosen randomly in the entire search space, a GA is globally oriented. Once, however, the global minimum is approached, the final convergence into the global minimum can be tediously slow because a GA does not exploit local information. Therefore, the final convergence is often carried out by a local search method (e.g. Wang 1991; Franchini 1996; Chelouah *et al.* 2000), which converges faster than a GA.

In this paper attention is focused on the optimization of nearshore process models with a GA, whose best solution after a given number of populations is used as a starting point for a local search with the downhill simplex method of Nelder & Mead (1965). Similar to a GA, the simplex method deals with a population of (albeit a limited number of) solutions but uses deterministic rules to find the global minimum. The aim of this work is to investigate the ability of the resulting hybrid algorithm, GA-SX, to find the optimum parameter values during the calibration of a three-parameter alongshore current model (Ruessink *et al.* 2001) and of the three-parameter cross-shore profile evolution model Unibest-TC (Bosboom *et al.* 1997). The alongshore current model is relatively simple, considering the amount of processes involved, and the three parameters show limited interaction. Unibest-TC is a more complex model and contains interdependent parameters. For each model the GA-SX is applied to a synthetic case, for which the global minimum is known and the model is an error-free representation, and to a measurement case, based on data collected during the 1998 Coast3D experiment at the double barred beach at Egmond aan Zee (Netherlands). Each time the effectiveness of the GA-SX algorithm is examined by running it five times with different initial populations. Finally, the main findings are discussed and summarized.

OPTIMIZATION

The use of an automatic optimization method requires the specification of the objective function, the algorithm and the termination criterion to decide whether or not convergence has been reached.

Objective function

The objective function adopted here is the Simple Least Squares function F, given by

$$F(\theta) = \sum_{x=1}^{N_x} \sum_{t=1}^{N_t} \left[X_{x,t}^{\text{obs}} - X_{x,t}^{\text{mod}}(\theta) \right]^2 \quad (1)$$

where θ is a vector of model parameters, N_x and N_t are the number of cross-shore (x) positions and moments in time t for which observations (X^{obs}) and model results (X^{mod}) are available. Note that F is dimensional and that its value depends on N_x and N_t. The minimum value $F(\theta)$ can attain is 0, in which case there is perfect agreement between X^{obs} and X^{mod} for all x and t.

Algorithm

The GA-SX algorithm comprises two successively applied search algorithms. It starts off with a genetic algorithm performing a global search through the feasible parameter search space to find a near-optimum solution. This solution is then further optimized using the local-search downhill simplex method of Nelder & Mead (1965). The principle of combining a globally oriented GA search to find the main area of interest with a local simplex search to converge to the global minimum was introduced by Wang (1991) and has recently been applied by Wolf & Moros (1997), Chelouah *et al.* (2000) and Chelouah & Siarry (2003). Our GA-SX algorithm differs from the existing algorithms in the selection and transformation rules used in the genetic algorithm.

Genetic algorithm

A genetic algorithm maintains a population of individuals at iteration i, $P(i) = \{p_1^i, \ldots, p_n^i\}$, where n is the number of individuals. Each individual p^i represents a potential solution to the global minimum. Based on the objective function value of each individual a new population (iteration $i + 1$) is selected from the more "fit" individuals, that is, the individuals having the lowest F. However, by chance, a poor individual may also be selected and a fit individual may be discarded; also, some individuals may be selected more than once. After the new population has been selected, some (randomly selected) individuals undergo transformations, known as crossover (mating) and mutation. It is hoped that the GA's "survival of the fittest" strategy and the subsequent transformations lead to a population whose individuals are closer to the desired global minimum than the individuals of the previous population. After the mutation step, the $(i + 1)$th iteration is complete. Then, the termination criterion is checked which, when satisfied, implies the end of the algorithm (and hands over the fittest individual of the last population to the simplex algorithm), or otherwise returns the population to the selection step to form a new population, etc.

In the present work a float representation (Michalewicz 1996) is used to describe each p^i, which implies that the actual real-number parameter values of θ make up the values of each p^i; this contrasts with the more traditional binary representation of p^i (Holland 1975). As shown by Michalewicz (1996), the float representation converges faster to a near-optimum solution than the binary representation, is more robust and provides a higher precision; also, it is intuitively more attractive to use than the binary coding because the value of the objective function is determined by parameters that are real numbers. For each parameter, a lower and upper bound is specified to outline the feasible space in which each parameter can vary.

Selection of the fitter individuals is here based on normalized geometric ranking (Houck *et al.* 1995). For each individual a measure of "fitness" is defined as the probability M that it is selected for the next population:

$$M = m'(1-m)^{r-1} \tag{2}$$

where m is the (user-specified) probability of selecting the best individual, r is the rank of the individual (where 1 is the best) and m' is the normalization factor given by

$$m' = m/[1-(1-m)^n]. \tag{3}$$

The actual selection of individuals is performed based on a comparison of the cumulative probability of M to a series of n sorted uniform random numbers between 0 and 1, see Houck *et al.* (1995) for further details. It is possible that an individual is selected more than once.

Now that a new population has been formed, some individuals will undergo crossover and mutation to guide the GA through the feasible parameter space to the global minimum. The intuition behind crossover is the exchange of information to find a near-optimum solution in an efficient way, whereas mutation serves to keep the population diverse, thereby avoiding early convergence in a local minimum. Here the crossover and mutation rules designed by Michalewicz (1996 pp 127–130) for float representations were implemented using a MATLAB tool developed by Houck *et al.* (1995).

The crossover rules are a set of three crossover operators (arithmetical, heuristic and simple crossover) which are run consecutively on the new individuals. In arithmetical crossover two individuals ("parents") are randomly selected and combined to yield two new individuals ("children") that take the place of their parents:

$$\begin{aligned}\theta_1' &= u\theta_1 + (1-u)\theta_2 \\ \theta_2' &= (1-u)\theta_1 + u\theta_2.\end{aligned} \tag{4}$$

In this equation, θ_1 and θ_2 are the parameter vectors of the two parents, θ_1' and θ_2' are the parameter vectors of the two children and u is a uniform random number between 0 and 1. In heuristic crossover a single child with parameter vector θ' is formed from two randomly selected parents as

$$\theta' = u(\theta_2 - \theta_1) + \theta_2 \tag{5}$$

where $F(\theta_2) \geq F(\theta_1)$. The child takes the place of the θ_2 parent. It is possible that θ' contains parameter values outside their bounds. In that case, a new u is generated until θ' is located in feasible parameter space. If heuristic crossover is still unsuccessful after five attempts, the crossover operator terminates and both parents remain in the population. In contrast to arithmetical crossover, heuristic crossover uses F information to guide the direction of the search. Finally, in simple crossover the parameter vectors of two randomly selected parents are crossed after the jth parameter, where j is a random integer number between 1 and the number of parameters N_p. Thus

$$\begin{aligned}\theta_1' &= \langle \theta_{1,1}, \ldots, \theta_{1,j}, \theta_{2,j+1}, \ldots, \theta_{2,N_p} \rangle \\ \theta_2' &= \langle \theta_{2,j}, \ldots, \theta_{2,j}, \theta_{1,j+1}, \ldots, \theta_{1,N_p} \rangle\end{aligned} \tag{6}$$

where $\langle\cdot\rangle$ denotes a vector. Arithmetical, heuristic and simple crossover were performed N_{c1}, N_{c2} and N_{c3} times, respectively.

The mutation rules are a set of three mutation operators (uniform, boundary and non-uniform mutation), again run successively on the new individuals (some of which, by now, are the result of crossover operations). In uniform mutation a randomly selected parameter from a randomly selected individual is replaced by a random value in the feasible space of the selected parameter. In boundary mutation a randomly selected parameter from a randomly selected individual takes the value of the lower bound of that parameter if u is less than 0.5 and of its upper bound if u is larger than or equal to 0.5. Finally, in non-uniform

mutation the jth randomly selected parameter of a randomly selected individual is adjusted as

$$\theta_j' = \begin{cases} \theta_j + (b_j - \theta_j)f(i) & \text{if } u_1 < 0.5 \\ \theta_j - (a_j + \theta_j)f(i) & \text{if } u_1 \geq 0.5 \end{cases} \quad (7)$$

where θ_j' is the adjusted value of the jth parameter, a_j and b_j are the lower and upper bound of θ_j, respectively, $f(i)$ is given by

$$f(i) = \left[u_2\left(1 - \frac{i}{i_{\max}}\right)\right]^2 \quad (8)$$

u_1 and u_2 are two uniform random numbers between 0 and 1, i is the current generation number and $i_{\max}$ is the maximum number of populations. In contrast to uniform mutation, non-uniform mutation invokes a global search of the GA when $i \ll i_{\max}$, turning into a local search when i is approaching $i_{\max}$ and, hopefully, all individuals have converged to the vicinity of the global minimum. Uniform, boundary and non-uniform mutation affected N_{m1}, N_{m2} and N_{m3} individuals, respectively.

Simplex algorithm

The "simplex" in the Nelder & Mead (1965) method is a geometric shape with $N_p + 1$ distinct vectors that are its vertices. In the three-parameter space of the present study, the simplex is a tetrahedron. After the initial simplex is formed using a step size equal to 5% of the parameter values provided by the GA, the simplex iteratively searches for the global minimum through a series of deterministic geometric transformations known as reflection, expansion, inside and outside contraction, and shrinkage. Because the downhill simplex algorithm is among the most often applied local search methods (because of its ease and robustness) it is not further described here. Instead, the interested reader is referred to Walters *et al.* (1991) and Lagarias *et al.* (1998). A graphical representation of the various geometric transformations for a simplex with four vertices (as is the case here) can be found in Chelouah *et al.* (2000).

Termination criteria

The global search with the genetic algorithm was terminated after a specified maximum number of generations $i_{\max}$. The subsequent local simplex search was ended when, for each parameter, the absolute difference in parameter value between the best and worst vertex was less than 0.001.

ALONGSHORE CURRENT MODELLING

Model

The alongshore current is a time-averaged (over ~3600 s) current that flows parallel to the coast and is forced by obliquely incident breaking waves, the alongshore component of the wind stress and 10–100 km scale alongshore surface slopes owing to tides. Its cross-shore distribution over an arbitrary cross-shore depth profile can be computed by solving the one-dimensional, time- and depth-averaged alongshore momentum balance, in which the three forcing terms balance with bottom stress and lateral mixing.

Here, the alongshore current model as proposed by Ruessink *et al.* (2001) is adopted. Measured offshore values of the root-mean-square wave height, wave period, wave angle, water level, alongshore wind stress and the large-scale sea-surface slope and a cross-shore depth profile are input into the model. A typical example of the predicted cross-shore structure of the alongshore current ($\bar{v}$) on a barred profile (as at Egmond aan Zee) is given in Figure 1 (offshore root-mean-square wave height = 1.5 m, wave period = 8 s and wave angle relative to shore normal = 30°, with no wind and no tidal forcing). As can be seen, the model produces current jets that are located at or on the shoreward side of each bar and near the shoreline (Figure 1). The magnitude of $\bar{v}$, the location of the maximum current of each jet ($\bar{v}_{\max}$) and the cross-shore width of each jet are determined by three parameters. The wave-front slope β influences the breaking-wave forcing; a decrease in β shifts the $\bar{v}_{\max}$ location onshore and broadens the current jet by increasing $\bar{v}$ in the trough (Figure 1(a)). The apparent bed roughness k_a, a parameter within the bottom stress formulation, affects the magnitude of $\bar{v}$ but does not alters the cross-shore shape of $\bar{v}$ (Figure 1(b)). The magnitude of the depth-averaged eddy viscosity ν determines the degree of lateral mixing, which smooths the cross-shore distribution of $\bar{v}$ without shifting the location of $\bar{v}_{\max}$ (Figure 1(c)).

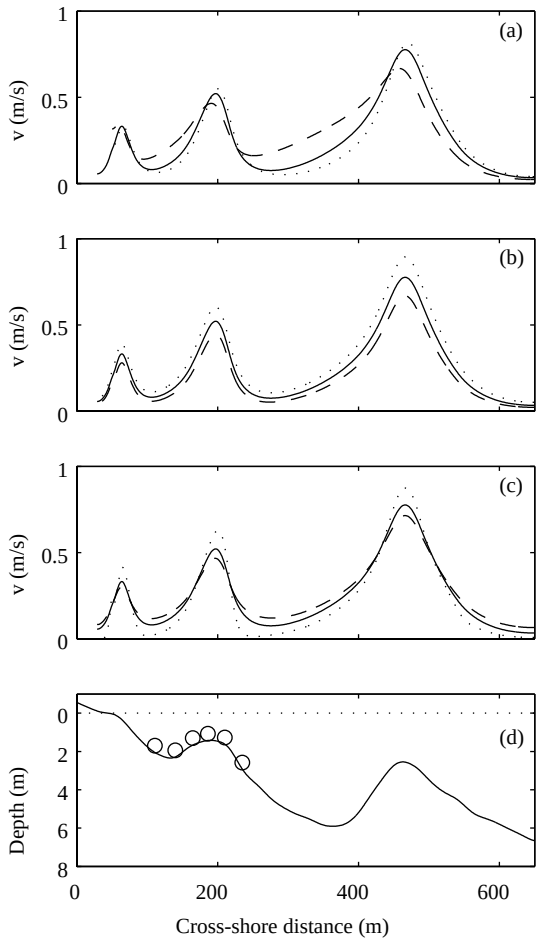

Figure 1 | Alongshore current $\bar{v}$ versus cross-shore distance showing the effect of changing the wavefront slope, apparent bed roughness and eddy viscosity. The solid curve in panels (a)–(c) is the standard run ($\beta = 0.1$, $k_a = 0.1$ m and $\nu = 0.5\,m^2/s$). Other curves correspond to changes in one parameter with the others held constant: (a) $\beta = 0.15$ (dotted line) and $\beta = 0.05$ (dashed line), (b) $k_a = 0.05$ m (dotted line) and $k_a = 0.2$ m (dashed line), (c) $\nu = 0\,m^2/s$ (dotted line) and $\nu = 1\,m^2/s$ (dashed line). (d) The depth profile was measured at Egmond on 15 October 1998. The shallow parts of the profile near cross-shore distances of 200 and 460 m are morphological features known as nearshore sandbars. The circles in (d) are the instrumented positions used in the optimization of the synthetic and measured $\bar{v}$ cases. The instrumented positions are labeled E1 to E6 from offshore to onshore.

Synthetic data

Synthetic 500 h $\bar{v}$ time series ($t = 107$–613 h in Figure 2) at the six instrumented Egmond positions (Figure 1(d)) were computed with $\beta = 0.08$, $k_a = 0.03$ m and $\nu = 0.5\,m^2\ s^{-1}$ using the input information measured during the Coast3D experiment (Figure 2), see Figure 3. In the synthetic data, the maximum $|\bar{v}|$ (in the cross-shore) ranges from $0.02\,m\ s^{-1}$ to $1.10\,m\ s^{-1}$ and is generally located just shoreward of the

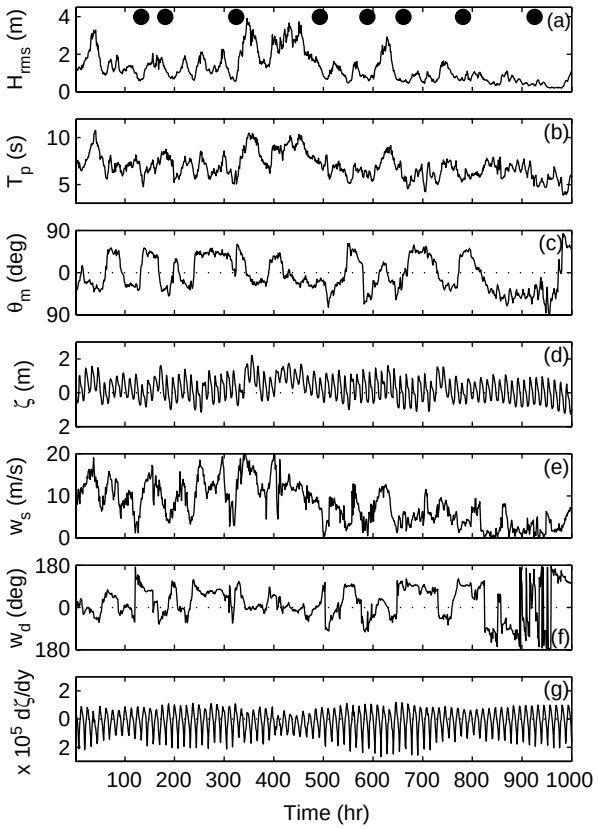

Figure 2 | (a) Offshore root-mean-square wave height H_{rms}, (b) offshore wave period T_p, (c) offshore wave angle θ_m relative to shore normal, (d) offshore water level ζ with respect to mean sea level, (e) wind speed w_s, (f) wind direction w_d relative to shore normal and (g) large-scale alongshore surface slope $d\zeta/dy$ versus time at Egmond. Time = 1 h corresponds to 11 October 1998, 00:00 MET. The black dots in (a) show the availability of depth profiles covering both the inner and outer bar.

bar crest at E3 or E4. The semi-diurnal variations in $\bar{v}$, most apparent at E1 and E6, are caused by semi-diurnal variations in the large-scale alongshore surface slope (Figure 2(g)).

An initial population of 30 individuals was generated by choosing θ randomly from a uniform distribution on the intervals [0.04, 0.12] for β, [0.015 m, 0.045 m] for k_a and $[0\,m^2\ s^{-1},\ 1\,m^2\ s^{-1}]$ for ν. The intervals for β and k_a are $\pm 50\%$ of their correct value, whereas the ν interval is $\pm 100\%$ of the correct value; this wider range reflect that model $\bar{v}$ is less sensitive to changes in ν than to changes in β or k_a. Values for the other parameters in the GA were $i_{max} = 10$, $m = 0.08$, $N_{c1} = N_{c2} = N_{c3} = 4$, $N_{m1} = N_{m2} = 4$ and $N_{m3} = 0$. In this way, the chance that the best individual is selected into the new population is 2.5 times as large as by pure chance; also, each new population has 20

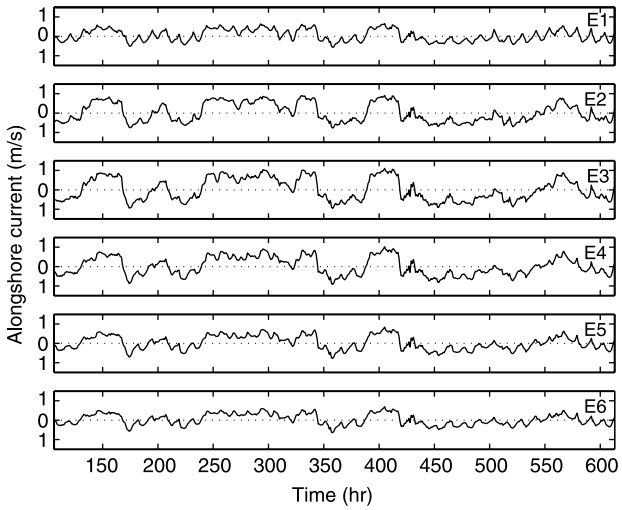

Figure 3 | Synthetic $\bar{v}$ from offshore (E1) to onshore (E6) versus time at Egmond.

new individuals formed through crossover (= 67% of total population, assuming all four heuristic crossovers to be successful) and eight parameter values are mutated (= 9% of all parameter values). Boundary mutation was not employed because it is known *a priori* that the correct values are within the feasible search space; boundary mutation may thus lead to unnecessary diversification when switched on. All numbers were experimentally chosen as representing a reasonable compromise between the constraints of population convergence and diversity, computing time and accuracy.

To test the effectiveness of the GA-SX algorithm, it was run five times, each time with a different initial population. Figures 4(a)–(c) show the GA convergence results of five trials. The mean $F(\theta)$, $\overline{F(\theta)}$, of each initial population varied between 6.7–10.1 $m^2\ s^{-2}$, with standard deviations σ between 5.9–11.2 $m^2\ s^{-2}$ (Figure 4(b)). The best individual had F values ($F_b(\theta)$) of 0.06–1.89 $m^2\ s^{-2}$ (Figure 4(c)). As the population number increased, most individuals evolved more and more to the main region around the global minimum: $\overline{F(\theta)}$ and σ decreased (Figures 4(a, b)), as did $F_b(\theta)$ (Figure 4(c)). Because of the uniform mutation operator σ did not reduce to 0 or close to 0 but varied around 0.5–1 $m^2\ s^{-2}$. In tests without this operator (and thus with non-uniform mutation only) σ decreased further to 0 (not shown).

In the 10th population the parameter values of the most fit individual were usually within 5–10% of their correct values. In all five trials, the subsequent downhill simplex algorithm converged in the global minimum. This 100% success ratio indicates the effectiveness of the GA-SX algorithm in finding the global minimum for the present synthetic data set. The average number of function calls (including the 30 calls required to initialize the first population and the calls made by the downhill simplex algorithm) amounted to 311.

Measurements

As for the synthetic current case, five initial populations with 30 individuals were generated, now sampled from a uniform distribution on the intervals [0.03, 0.1] for β, [0.005 m, 0.1 m] for k_a and [0 $m^2\ s^{-1}$, 2 $m^2\ s^{-1}$] for ν. The GA variables were set to the same values as in the synthetic current case, except for N_{m3}, which was set to 4. This increased the number of parameters mutated in each population to 12 (= 13% of all parameters). The data to which the model predictions were compared comprise ~500 h time series (t = 107–613 h in Figure 2) measured at the six instrumented positions at Egmond (Figure 1(d)) during the Coast3d experiment.

As can be seen in Figures 4(d, e), $\overline{F(\theta)}$ in the first population varied between 74.7–85.7 $m^2\ s^{-2}$, with standard deviations between 14.5–18.7 $m^2\ s^{-2}$. These $\overline{F(\theta)}$ are substantially higher than in the synthetic current case because now both the model and the data contain errors. In all five initial populations $F_b(\theta)$ already outperformed the best $F(\theta)$ determined manually by Ruessink *et al.* (2001), see Figure 4(f). This implies that a pure random search (Brooks 1958) with 30 different θ guesses already results in a θ estimate closer to the global minimum than an extensive manual calibration in which each parameter is varied one at a time.

As the GA moved from population to population, $\overline{F(\theta)}$ and $F_b(\theta)$ further reduced (Figures 4(d, f)). In contrast, σ typically remained rather high (Figure 4(e)), caused by the boundary mutation operator. All five simplex runs converged at $\beta = 0.055$, $k_a = 0.026$ m and $\nu = 1.30\ m^2\ s^{-1}$, implying this to be the global optimum θ. In the optimum, F amounted to 55.65 $m^2\ s^{-2}$, about 5.5% lower than the manually determined F of 58.9 $m^2\ s^{-2}$. The average amount of function calls was 357. The measured and best-fit modelled $\bar{v}$ are shown in Figure 5.

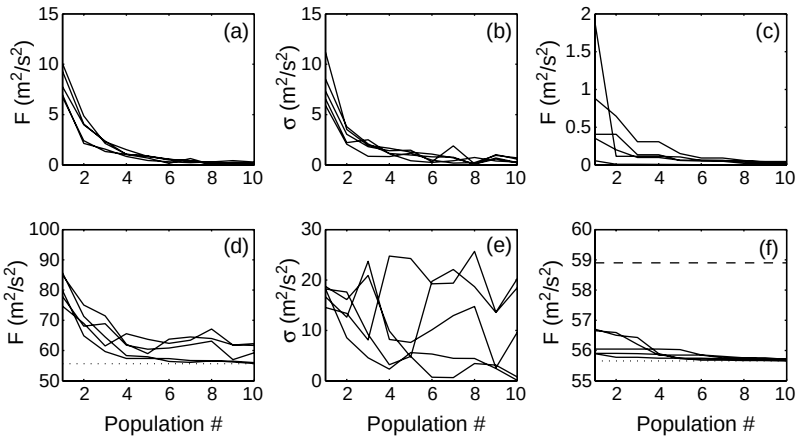

Figure 4 | Convergence of the genetic algorithm for the synthetic (top) and measured (bottom) $\bar{v}$ data. (a), (d) the population-mean objective function value $\overline{F(\theta)}$ versus population number; (b), (e) the standard deviation of the objective function value versus population number; and (c), (f) the objective function value of the best individual $F_b(\theta)$ versus population number. The five lines in each plot correspond to the results of five replications started with a different stage of the random generator. The dotted lines in (d) and (f) correspond to F in the global minimum; the dashed line in (f) is the F determined manually by Ruessink *et al.* (2001).

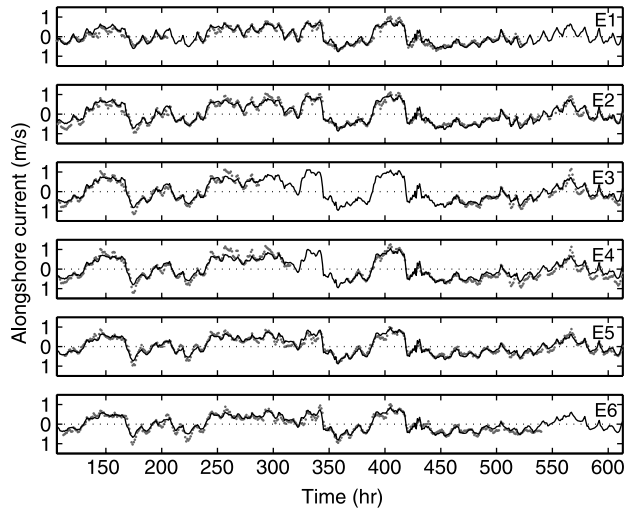

Figure 5 | Measured (symbols) and modelled (lines, $\beta = 0.055$, $k_a = 0.026$ m and $\nu = 1.30\,m^2\,s^{-1}$) $\bar{v}$ from offshore (E1) to onshore (E6) versus time at Egmond.

CROSS-SHORE PROFILE MODELLING

Model description

A cross-shore profile evolution model aims at predicting cross-shore bathymetric evolution by accounting explicitly for the various hydrodynamical and sediment transport processes involved. A hydrodynamical module computes the cross-shore wave height and current distributions, which are subsequently used as local input into sediment transport equations. Morphological changes are then calculated from the cross-shore gradients in the time-averaged sediment transport rates, after which the procedure is repeated. For a depth profile with sandbars, like at Egmond (Figure 1(d)), a profile evolution model essentially aims to predict the correct temporal evolution of the sandbars (i.e. their position, width and height). The model used in the following is the commercially available 2.04d-v1 version of Unibest-TC (Bosboom *et al.* 1997; Van Kessel 2000; Walstra 2000), developed by WL|Delft Hydraulics (Netherlands). A full description of the model equations can be found in Bosboom *et al.* (1997). An initial cross-shore depth profile and time series of offshore values of the root-mean-square wave height, wave period, wave angle, water level, wind speed and direction, and large-scale sea-surface slope are input into Unibest-TC.

The model contains 15 free parameters. Earlier work, using wave heights and mean currents measured in the laboratory and the field, has resulted in the operational assumption that the parameters in the wave and current modules need not be optimized for every new application and can thus be kept constant at their default values (Walstra 2000). In this study the values of the three uncertain parameters in the sediment transport module are optimized. In Unibest-TC the cross-shore sediment transport rate is the sum of the bedload transport rate and the current-related suspended load transport rate. The latter

rate, which inside the surfzone dominates over the bedload transport rate, involves the computation of the vertical equilibrium concentration profile using the time-averaged convection–diffusion equation, for which the approach outlined in Van Rijn (1993) is adopted. The convection–diffusion equation is solved by numerical integration from a near-bed reference level to the water surface; at the reference level a reference concentration is specified as boundary condition (Van Rijn 1993).

The first free parameter optimized here, referred to as the current-related roughness k_c, determines the height of the near-bed reference level. An increase in k_c increases this level, which reduces the reference concentration and, accordingly, the current-related suspended sediment transport rate. Under storm conditions, when cross-shore mean currents are offshore directed, an increase in k_c thus results in a reduced offshore bar migration (Figure 6(a)). An increase in the second free parameter, the wave-related roughness k_w, increases the near-bed wave-related bed shear stress, which in turn leads to an increase in the reference concentration and the current-related suspended sediment transport rate. Under storm conditions an increase in k_w causes a bar to migrate further in the offshore direction (Figure 6(b)). Obviously, k_c and k_w are interdependent because both parameters affect the current-related suspended sediment transport rate through the reference concentration. The third free parameter, the tangent of the angle of repose tan ϕ, affects bed level prediction through the bedload formulations, in which it determines the threshold criterion for the initiation of motion and plays a role in the gravity-induced transport. In both cases, a decrease in tan ϕ hinders upslope transport and stimulates downslope transport: in other words, smears out the existing bars (Figure 6(c)). Its effect on bar position is minimal. Tests suggest (not shown) that the bedload transport rate becomes insensitive to tan ϕ for tan ϕ larger than 0.25–0.30.

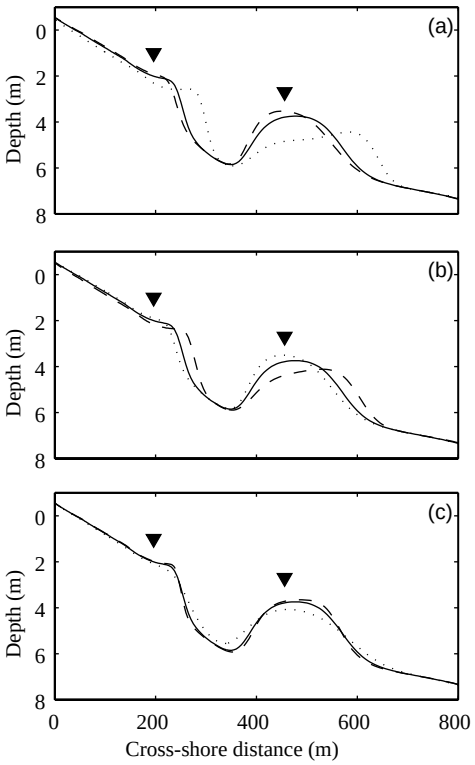

Figure 6 | Predicted bed levels after 16 days of storms (Figure 2, $t = 133$–517 h) at Egmond showing the effect of changing the current-related roughness, wave-related roughness and angle of repose. In each case, the profile in Figure 2(d) was used as the initial depth profile; the triangles in each panel reflect the position of the outer and inner bar in this initial profile. The solid curve in panels (a)–(c) is the standard run ($k_c = 0.03$ m, $k_w = 0.01$ m and tan $\phi = 0.2$). Other curves correspond to changes in one parameter with the others held constant: (a) $k_c = 0.01$ m (dotted line) and $k_c = 0.05$ m (dashed line), (b) $k_w = 0.003$ m (dotted line) and $k_w = 0.03$ m and (c) tan $\phi = 0.1$ (dotted line) and tan $\phi = 0.3$ (dashed line).

Synthetic data

Synthetic data (Figure 7) were generated with $k_c = 0.03$ m, $k_w = 0.01$ m and tan $\phi = 0.2$ using the waves and tides measured during the 33-d Coast3D period (Figure 2, $t = 133$–925 h) and a median grainsize of 240 μm. The model, initialized with the cross-shore profile measured at $t = 133$ h, was run with a time step of 0.5 h on a grid with a distance between consecutive points reducing from 5 m across the outer bar to 1 m on the beach. Modelled cross-shore depth profiles were stored for the same seven moments for which measured profiles also exist (Figure 2). In the synthetic data the crest of the inner bar moves offshore by about 30 m during the first 15 d, after which it moves onshore by about 12 m; note how the inner bar-trough relief vanishes altogether in the synthetic data (Figure 7). The outer bar has shifted offshore by about 10–15 m at $t = 15$ d; at the same time, the outer bar-trough relief has become more subdued (Figure 7).

The GA variables were chosen identical to the synthetic $\bar{v}$ case. The initial population of 30 individuals was sampled

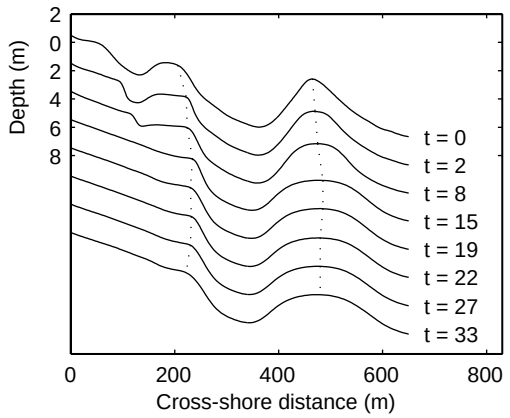

Figure 7 | Synthetic bed evolution data set. The time stamp refers to the number of days after the initial depth profile. Each consecutive profile is offset by an additional 2 m. The dotted lines connect the inner and outer bar crest positions, respectively.

from a uniform distribution on the intervals [0.005 m, 0.02 m] for k_w, [0.02 m, 0.04 m] for k_c and [0.1, 0.25] for tan ϕ, chosen because of the recommendations in Walstra (2000). Values of the objective function were computed using depth values on the interval $130 < x < 600$ m (seaward side of the outer bar up to and including the inner trough), not including the initial depth profile. Again, the GA-SX algorithm was run 5 times with a different initial population to test its effectiveness in finding the true parameter values.

Figures 8(a)–(c) show the convergence results of the genetic algorithm. In each of the 5 trials, $F_b(\theta)$ in the final population was less than 0.1 m^2, implying the modelled depth profiles to be essentially indistinguishable from the synthetic profiles. The value of tan ϕ in the best parameter vector in the final population equalled 0.2 in each trial; however, k_c and k_w could still be up to 30% from their correct values. In none of the 5 trials did the downhill simplex method succeed in reducing F to 0, or even in moving k_c or k_w towards their correct values.

As can be seen in Figure 9, the k_c and k_w values at termination were located on the floor of a deep and elongated valley in the error surface, caused by k_c–k_w interaction in the computation of the current-related suspended sediment transport rate (cf. Johnston & Pilgrim 1976; Gupta & Sorooshian 1983; Kirkby *et al.* 1993). Even though the error surface is unimodal, there is a disturbing range of k_c–k_w possibilities that result in a near-zero F. It appears that once the genetic algorithm has found a parameter vector on the main axis of the error valley, neither additional crossover and mutation operations nor the downhill simplex method are capable of producing a better parameter vector (obviously, one can also argue that any pair of k_c and k_w on the floor of the error valley is as good as any other from a mathematical point of view as they all have an F of approximately 0). Thus, even in the case of error-free (synthetic) data the poor properties of the response surface prohibit the GA-SX algorithm from obtaining the correct and unique parameter set.

The natural question that now may be raised is how the failure of the GA-SX algorithm to locate the global minimum can be repaired. Because the failure is caused by the model

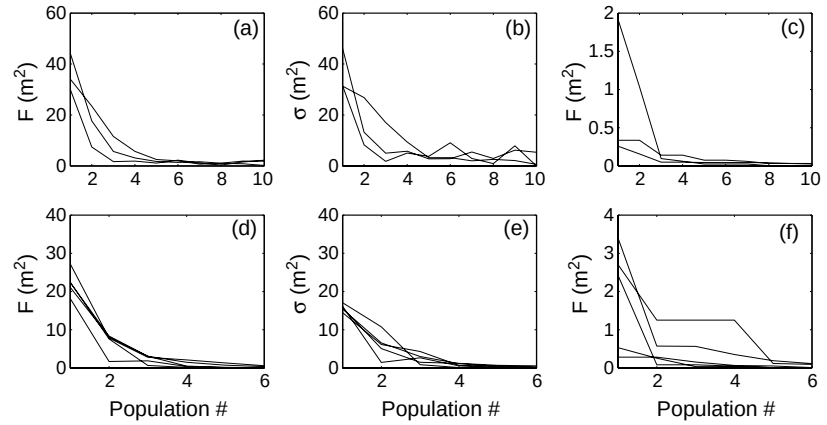

Figure 8 | Convergence of the genetic algorithm for the synthetic $\bar{z}$ data. (a) The population-mean objective function value $\overline{F(\theta)}$ versus population number, (b) the standard deviation of the objective function value versus population number and (c) the objective function value of the best individual $F_b(\theta)$ versus population number. Plots (d)–(f) show the same as (a)–(c) but now with $k_c = 0.03$ m. The five lines in each plot correspond to the results of five replications started with a different stage of the random generator.

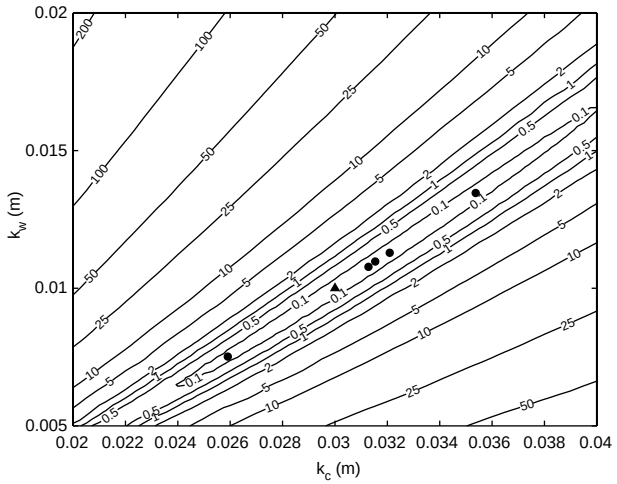

Figure 9 | Contour plot of the objective function F for the synthetic bathymetric data as a function of the current-related roughness k_c and the wave-related roughness k_w (tan $\phi = 0.2$). The triangle is located at the known optimum, $k_c = 0.03$ m and $k_w = 0.01$ m. The circles are the solutions of the GA-SX algorithm.

structure, it cannot be expected that much improvement over what is already achieved so far will be obtained by changing the settings in the GA-SX algorithm or by using another optimization algorithm. Sorooshian & Gupta (1983) were faced with a similar ill-posed optimization problem in the representation of percolation in a conceptual watershed model, motivating Gupta & Sorooshian (1983) to alter this representation to make its two involved parameters independent. However, as pointed out by Kirkby *et al.* (1993), a change in the model structure should only be carried out when there are sound physical reasons for requiring the parameters to be independent. Otherwise, a simple solution is to fix one of the two parameters within its feasible space while retaining the other in the optimization procedure. A potential drawback of this choice is that when other parameters depend on either of the two interdependent parameters, their optimum values may differ from the correct values as a result of compensating changes necessary to minimize the error caused by assuming one of the free parameters to be constant (Sorooshian & Gupta 1983). This does not appear to be the case here as, irrespective of where the GA-SX algorithm converged in the error valley, it always produced the correct tan ϕ. Other drawbacks are that it may not be *a priori* clear which parameter must be fixed and the choice of its value is, to some extent, subjective. Another solution is to extend the objective function of (1) with a regularization term $F_r(\theta)$ of the form

$$F_r(\theta) = 0.5(\theta - \theta_0)^T \Gamma^{-1}(\theta - \theta_0) \quad (9)$$

in which θ_0 is a best prior estimate of the parameter vector θ and Γ is a covariance matrix that represents the uncertainty in θ. With this regularization a well-posed optimization solution can be obtained without the necessity to remove one of the uncertain parameters. The final θ estimate is now a mix of the prior estimate and the agreement of model predictions and observations. However, just as with the fixation of a single parameter, the choice of θ_0 and Γ is rather subjective.

Here, the suggested improvement to the Unibest-TC optimization problem is the fixation of k_c to 0.03 m. In this way, the near-bed reference height required in the computation of the current-related suspended sediment transport rate is fixed to the middle of its feasible range. The GA-SX algorithm was then run five times with k_w and tan ϕ sampled initially from the same distribution as before. The genetic algorithm settings were $n = 15$, $i_{max} = 6$, $m = 0.17$, $N_{c1} = N_{c2} = N_{c3} = 3$, $N_{m1} = 2$, $N_{m2} = 1$ and $N_{m3} = 0$. Note that n and i_{max} were reduced because now only two parameters are involved in the calibration procedure; values of the remaining parameters were adjusted to have approximately the same chances of selection, crossover and mutation as in the previous three-parameter calibration. Each time (Figures 8(d)–(f)) $F_b(\theta)$ in the sixth population was approximately 0 based on k_w and tan ϕ values within 4% of their correct values. All five simplex runs subsequently produced $k_w = 0.01$ m and tan $\phi = 0.2$. Thus, setting k_c to a constant value within its feasible space has "solved" the Unibest-TC optimization problem and led to a 100% success ratio. The average number of function calls amounted to 108.

Measurements

Existing comparisons (Van Rijn *et al.*, 2003) of model predictions against the seven depth profiles measured during the Egmond Coast3D campaign (Figure 2, $t = 133$–925 h) are based on $k_c = 0.03$ m, $k_w = 0.01$ m and tan $\phi = 0.1$. This setting (with the same grid and time step as in the previous synthetic case) results in $F = 224.4$ m^2 on the interval $130 < x < 600$ m (seaward side of the outer bar

up to and including the inner trough), not including the initial depth profile.

Figure 10 shows the GA convergence results based on $k_c = 0.03\,\text{m}, n = 15, i_{\max} = 6, m = 0.17, N_{c1} = N_{c2} = N_{c3} = 3$ and $N_{m1} = N_{m2} = N_{m3} = 1$. It is intriguing to see that in each of the five initial populations $\overline{F(\theta)}$ already outperformed the manually determined F, again showing that a simple random sampling of the free parameters in their feasible space can result in a lower F than one based on a manual calibration in which each parameter is varied at a time. Each of the five trials terminated near $F = 135\,\text{m}^2$ with optimum $k_w = 0.011\,\text{m}$ and $\tan\phi = 0.25$. Thus, the optimum k_w was very close (relative to the width of its feasible space) to the manually determined k_w, but the optimum $\tan\phi$ was 2.5 times as large as the manual $\tan\phi$. The number of function calls required to reach the optimum values amounted to 111 (averaged over the five trials). Measured and modelled best-fit depth profiles are shown in Figure 11. Note that the model smooths the outer bar more than was observed in the measurements (especially from $t = 8$–$15\,\text{d}$) and that the model predicts too much erosion on the beach, causing a shoreward infilling of the inner trough (compare modelled profiles at $t = 2$ and $t = 8\,\text{d}$) and its complete disappearance at $t = 15\,\text{d}$.

DISCUSSION

In this paper the effectiveness of the globally oriented GA-SX algorithm in finding optimum parameter settings was examined using synthetic and measured alongshore current and bed profile evolution data. Whereas the algorithm was an effective method to calibrate the alongshore current model, it failed to identify the optimum parameter values in the bed evolution model using error-free synthetic data, related to the strong interaction between two of the parameters in the suspended sediment transport equation. Fixing one of the interdependent parameters to a constant value within its feasible space while retaining the other in the optimization procedure proved to be an effective solution to the ill-posed optimization problem of the bed evolution model. In the following the efficiency of the GA-SX algorithm is examined by comparing the required number of function calls to that required by a multistart simplex method; also, the uncertainties in the parameter estimates are discussed.

Efficiency

The motivation for the genetic algorithm was its probabilistic information sharing methodology in maintaining a population of solutions, a more efficient method than a multistart method comprising independent local searches. In order to see how much is gained by information sharing, a total of 4 multistart runs with 15 simplexes each was performed, one for each synthetic and measured alongshore current and depth profile case, respectively. The initial parameter guess for each simplex was chosen randomly from the same feasible space as in the GA-SX applications. In each multistart run, all simplexes converged into the same parameter set as found by the GA-SX algorithm. However, as can be deduced from Table 1, the amount of required function calls exceeded that of the GA-SX algorithm by at least a factor of 5 (note that in the two $\bar{v}$ runs the amount of simplexes was only half the number of individuals in a population). This demonstrates the efficiency of the GA-SX algorithm in finding the global optimum by information sharing.

The 100% effectiveness of each multistart run implies that the response surfaces of the alongshore current and bed

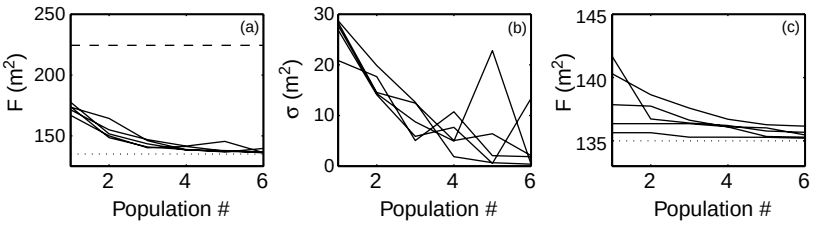

Figure 10 | Convergence of the genetic algorithm for the measured depth data based on $k_c = 0.03\,\text{m}$. (a) The population-mean objective function value $\overline{F(\theta)}$ versus population number, (b) the standard deviation of the objective function value versus population number and (c) the objective function value of the best individual $F_b(\theta)$ versus population number. The five lines in each plot correspond to the results of five replications started with a different stage of the random generator. The dotted lines in (a) and (c) correspond to F in the global minimum; the dashed line in (a) is the manually determined F (Van Rijn *et al.*, 2003).

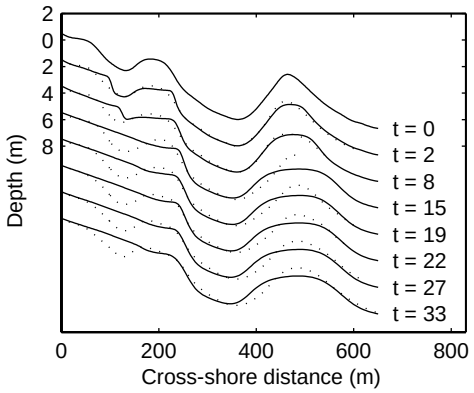

Figure 11 | Measured (dotted lines) and modelled (solid lines, $k_c = 0.03$ m, $k_w = 0.011$ m and $\tan\phi = 0.25$) bed evolution data set. The time stamp refers to the number of days after the initial depth profile. Each consecutive profile is offset by an additional 2 m.

profile evolution models are most likely unimodal. In hindsight, one could therefore argue that the global nature of the GA-SX was overdone and that a single run of a local search method would have sufficed. However, the GA-SX algorithm required, on average, about three times as many function calls as only a single simplex run (Table 1). In my opinion, this is a small price to pay for a higher guarantee that the correct parameter values have been found.

The ratios given above should not be taken too literally. The GA method contains some arbitrary and intuitive settings, such as the size of the population, the number of crossovers and mutations, and the order in which the various operators are performed. As mentioned earlier, some experiments were carried out to ensure that the population remained sufficiently diverse to prevent a premature convergence on the best member of the first population and to avoid excessive (more than several days for a single trial) computing time. There is still a potential to improve the GA's efficiency by optimizing its settings. Also, the convergence rate of the simplex algorithm may be improved by optimizing the step size to form the initial simplex (Walters *et al.*, 1991).

Table 1 | Number of function calls

	Synthetic		Measured	
Algorithm	**Current**	**Depth**	**Current**	**Depth**
GA-SX	311	108	357	111
Multistart SX	1446	570	2104	603

Parameter accuracy

Any optimal parameter solution is more meaningful if the uncertainties in the parameter estimates can be quantified. The posterior description of parameter uncertainty can be used, for instance through Monte Carlo simulation, to produce probabilistic model forecasts. The GA-SX algorithm does not produce uncertainty information about the optimal solution; accordingly, alternative methods are needed to acquire this information. One potential method is to use multiple calibration periods. Each period will, no doubt, produce different optimum parameter sets, whose distribution would reflect the uncertainty in the parameter estimates. Multiple calibration periods can be constructed via resampling techniques (e.g. Van den Boogaard *et al.* 2000) or, more simply, by dividing one extensive calibration periods into several parts (e.g. Beven 1993), where each part should obviously still contain sufficient different conditions for calibrating the parameters. As pointed out by Sorooshian *et al.* (1983) and Gan & Biftu (2003), the information content in the calibration time series rather than its length determines the success of an optimization algorithm in finding the correct values.

The extension to multiple calibration periods to estimate uncertainty information was, as an example, applied to the alongshore current model by dividing the available Egmond data into ten 50 h (roughly the duration of a storm) periods. The optimum parameter setting for each subperiod was then determined with a single GA-SX run with the same settings as before. The mean ± 1 standard deviation for β, k_a and ν were 0.057 ± 0.029, 0.023 ± 0.007 m and 1.44 ± 0.94 m^2 s^{-1}, respectively.

CONCLUSIONS

Based on synthetic and measured alongshore current and bed evolution data the globally oriented GA-SX algorithm, combining a population-evolution-based search strategy and a Nelder–Mead downhill simplex search, is found to be an effective and efficient (relative to a multistart simplex run) tool to find optimum parameter

settings in nearshore process models. Essential to the effectiveness of the algorithm is the absence of interdependent free parameters which, consistent with earlier work in watershed modelling (e.g. Johnston & Pilgrim 1976; Gupta & Sorooshian 1983), frustrate calibration by creating a deep, elongated and flat-bottomed valley in the error surface and result in widely varying parameter settings with virtually the same error. Setting one of the interdependent parameters to a constant value within its feasible space while retaining the other in the optimization procedure is found to be a feasible solution to such an ill-posed optimization problem.

ACKNOWLEDGEMENTS

I am greatly indebted to Dirk-Jan Walstra (WL|Delft Hydraulics, Delft, Netherlands) for providing me with the Unibest-TC software and for answering all my questions on profile modelling. Robert T. Guza's (Scripps Institution of Oceanography, San Diego, CA, USA) remarks on the usefulness of manual calibration during our work on the modelling of alongshore currents started my interests in automated calibration algorithms. The constructive comments from one of the anonymous reviewers are also acknowledged.

REFERENCES

Beven, K. 1993 Prophecy, reality and uncertainty in distributed hydrological modelling. *Adv. Wat. Res.* **16**, 41–51.

Bosboom, J., Aarninkhof, S. G. J., Reniers, A. J. H. M., Roelvink, J. A. & Walstra, D. J. R. 1997 Unibest-TC 2.0. Overview of model formulations., *Report* H2305.42, WL|Delft Hydraulics.

Brooks, S. H. 1958 A discussion of random methods for seeking maxima. *Oper. Res.* **6**, 244–251.

Chelouah, R. & Siarry, P. 2003 Genetic and Nelder-Mead algorithms hybridized for a more accurate global optimization of continuous multiminima functions. *Eur. J. Oper. Res.* **148**, 335–348.

Chelouah, R., Siarry, P., Berthiau, G. & De Barmon, B. 2000 An optimization method fitted for model inversion in non destructive control by eddy currents. *Eur. Phys. J. Appl. Phys.* **12**, 231–238.

Duan, Q. 2003 Global optimization for watershed model calibration. In *Calibration of Watershed Models* (ed. Q. Duan, H. V. Gupta, S. Sorooshian, A. N. Rousseau & R. Turcotte). AGU, Washington, pp. 89–104.

Duan, Q., Sorooshian, S. & Gupta, V. 1992 Effective and efficient global optimization for conceptual rainfall-runoff models. *Wat. Res. Res.* **28**, 1015–1031.

Franchini, M. 1996 Using a genetic algorithm combined with a local search method for the automatic calibration of conceptual rainfall-runoff models. *Hydrol. Sci. J.* **41**, 21–40.

Gan, T. Y. & Biftu, G. F. 2003 Effects of model complexity and structure, parameter interactions and data on watershed modeling. In *Calibration of Watershed Models* (ed. Q. Duan, H. V. Gupta, S. Sorooshian, A. N. Rousseau & R. Turcotte). AGU, Washington, pp. 317–328.

Gupta, V. K. & Sorooshian, S. 1983 Uniqueness and observability of conceptual rainfall-runoff model parameters: the percolation process examined. *Wat. Res. Res.* **19**, 269–276.

Holland, J. H. 1975 *Adaptation in Natural and Artificial Systems*. University of Michigan Press, Ann Arbor, MI.

Houck, C. R., Joines, J. R., & Kay, M. G. 1995 A genetic algorithm for function optimization: a Matlab implementation. *Technical Report* NCSU-IE-TR-95-09, North Carolina State University, Raleigh, NC

Johnston, P. R. & Pilgrim, D. H. 1976 Parameter optimization for watershed models. *Wat. Res. Res.* **12**, 477–486.

Kirkby, M. J., Naden, P. S., Burt, T. P. & Butcher, D. P. 1993 *Computer Simulation in Physical Geography*. John Wiley & Sons, Chichester.

Lagarias, J. C., Reeds, J. A., Wright, M. H. & Wright, P. E. 1998 Convergence properties of the Nelder-Mead Simplex method in low dimensions. *SIAM J. Optimiz.* **9**, 112–147.

Michalewicz, Z. 1996 *Genetic Algorithms + Data Structures = Evolution Programs*. Springer Verlag, Berlin.

Nelder, J. A. & Mead, R. 1965 A simplex method for function minimization. *Comput. J.* **7**, 308–313.

Ruessink, B. G., Miles, J. R., Feddersen, F., Guza, R. T. & Elgar, S. 2001 Modeling the alongshore current on barred beaches. *J. Geophys. Res.* **106**, 22451–22463.

Ruessink, B. G., Walstra, D. J. R. & Southgate, H. N. 2003 Calibration and verification of a parametric wave model on barred beaches. *Coastal Engng.* **48**, 139–149.

Sorooshian, S. & Gupta, V. K. 1983 Automatic calibration of conceptual rainfall-runoff models: the question of parameter observability and uniqueness. *Wat. Res. Res.* **19**, 260–268.

Sorooshian, S., Gupta, V. K. & Fulton, J. L. 1983 Evaluation of maximum likelihood parameter estimation techniques for conceptual rainfall-runoff models: influence of calibration data variability and length on model credibility. *Wat. Res. Res.* **19**, 251–259.

Van den Boogaard, H. F. P., Mynett, A. E. & Heskes, T. 2000 Resampling techniques for the assessment of uncertainties in parameters and predictions of calibrated models. *Proc. Hydroinformatics '00*, University of Iowa, CD-ROM.

Van Kessel, T. 2000 Unibest v204 documentation. *Report* Z2899.40, WL|Delft Hydraulics

Van Rijn, L. C. 1993 Principles of Sediment Transport in Rivers, Estuaries and Coastal Seas. AQUA Publications, Amsterdam.

Van Rijn, L. C., Walstra, D. J. R., Grasmeijer, B., Sutherland, J., Pan, S. & Sierra, J. P. 2003 The predictability of cross-shore bed evolution of sandy beaches at the time scale of storms and seasons using process-based profile models. *Coastal Engng.* **47**, 295–327.

Walstra, D. J. R. 2000 Unibest-TC user guide. *Report* Z2897, WL|Delft Hydraulics.

Walters, F. H., Morgan, S. L., Parker, L. R. & Deming, S. N. 1991 *Sequential Simplex Optimization*. CRC Press, Boca Raton, FL.

Wang, Q. J. 1991 The genetic algorithm and its application to calibrating conceptual rainfall-runoff models. *Wat. Res. Res.* **27**, 2467–2471.

Wolf, D. & Moros, R. 1997 Estimating rate constants of heterogeneous catalytic reactions without supposition of rate determining surface steps – an application of a genetic algorithm. *Chem. Engng. Sci.* **52**, 1189–1199.